

Monte Carlo sampling for stochastic weight functions

Daan Frenkel^{a, 1}, K. Julian Schrenk^a, and Stefano Martiniani^a

^aDepartment of Chemistry, University of Cambridge, Lensfield Road, Cambridge, CB2 1EW, United Kingdom

This manuscript was compiled on May 18, 2017

Conventional Monte Carlo simulations are stochastic in the sense that the acceptance of a trial move is decided by comparing a computed acceptance probability with a random number, uniformly distributed between 0 and 1. Here we consider the case that the weight determining the acceptance probability itself is fluctuating. This situation is common in many numerical studies. We show that it is possible to construct a rigorous Monte Carlo algorithm that visits points in state space with a probability proportional to their average weight. The same approach may have applications for certain classes of high-throughput experiments and for the analysis of noisy datasets.

Markov chain Monte Carlo | Configurational bias | Basin volume | Transition state finding

Monte Carlo simulations aim to sample the states of the system under study such that the frequency with which a given state is visited is proportional to the weight (often ‘Boltzmann’ weight) of that state. The equilibrium distribution of a system, i.e. the distribution for which every state occurs with a probability proportional to its (Boltzmann) weight, is invariant under application of single Monte Carlo step. Algorithms that satisfy this criterion are said to satisfy ‘balance’ (1). Usually, we impose a stronger condition: ‘detailed balance’, which implies that the average rate at which the system makes a transition from an arbitrary ‘old’ state (o) to a ‘new’ state (n) is exactly balanced by the average rate for the reverse rate. The detailed balance condition is a very useful tool to construct valid Markov Chain Monte Carlo (MCMC) algorithms. We can write the detailed balance condition as follows;

$$P(\mathbf{x}_o)P_{\text{gen}}(o \rightarrow n)P_{\text{acc}}(o \rightarrow n) = P(\mathbf{x}_n)P_{\text{gen}}(n \rightarrow o)P_{\text{acc}}(n \rightarrow o) \quad [1]$$

where $P(\mathbf{x}_i)$ denotes the equilibrium probability that the system is in state i (in this case, i can stand for o or n) characterised by a (usually high-dimensional) coordinate \mathbf{x}_i . $P_{\text{gen}}(i \rightarrow j)$ denotes the probability to generate a trial move from state i to state j . In the simplest case, this may be the probability to generate a random displacement that will move the system from \mathbf{x}_i to \mathbf{x}_j , but in general the probability to generate a trial move may be much more complex (see e.g. Ref. (2)). Finally $P_{\text{acc}}(i \rightarrow j)$ denotes the probability that a trial move from state i to state j will be accepted.

Many simple MC algorithms satisfy in addition microscopic reversibility, which means that $P_{\text{gen}}(i \rightarrow j) = P_{\text{gen}}(j \rightarrow i)$. In that case, detailed balance implies that

$$\frac{P_{\text{acc}}(o \rightarrow n)}{P_{\text{acc}}(n \rightarrow o)} = \frac{P(\mathbf{x}_n)}{P(\mathbf{x}_o)} \quad [2]$$

There are many acceptance rules that satisfy this criterion.

The most familiar one is the so-called Metropolis rule (3):

$$P_{\text{acc}}(o \rightarrow n) = \text{Min} \left\{ 1, \frac{P(\mathbf{x}_n)}{P(\mathbf{x}_o)} \right\} \quad [3]$$

The acceptance probability for the reverse move follows by permuting o and n . In the specific case of Boltzmann sampling of configuration space, where the equilibrium distribution is proportional to the Boltzmann factor $P(\mathbf{x}_i) \sim \exp(-U_i/k_B T)$, where U_i is the potential energy of the system in the state characterised by the coordinate \mathbf{x}_i , T is the absolute temperature and k_B is the Boltzmann constant. In that case, we obtain the familiar result

$$P_{\text{acc}}(o \rightarrow n) = \text{Min} \{ 1, \exp[-(U_n - U_o)/k_B T] \} \quad [4]$$

Monte Carlo simulations with ‘noisy’ acceptance rules.

There are many situations where conventional MCMC cannot be used because the quantity that determines the weight of a state i is, itself, the average of a fluctuating quantity. Specifically, we consider the case of weight functions fluctuating according to a Bernoulli process, i.e. in an intermittent manner, although our approach is not limited to Bernoulli processes. Examples that we consider are ‘committor’ functions, or the outcome of a stochastic minimisation procedure.

Note that the problem that we are discussing here is different from the cases considered by Bhanot and Kennedy (4) and by Ceperley and Dewing (5). As we will discuss below, these earlier papers consider cases where the weights are non-linear functions of a fluctuating argument (e.g. an action or

Significance Statement

Markov Chain Monte Carlo is the method of choice for sampling high-dimensional (parameter) spaces. The method requires knowledge of the weight function (or likelihood function) determining the probability with which a states is observed. Yet, in many numerical applications the weight function itself is fluctuating. Here we present a new approach capable of tackling this class of problems by rigorously sampling states proportionally to the average value of their fluctuating likelihood. We demonstrate that the method is capable of computing the volume of a basin of attraction defined by stochastic dynamics, as well as being an efficient method to identify a transition state along a known reaction coordinate. We briefly discuss how the method might be extended to experimental settings.

D. F. and S. M. contributed to all aspects of research and wrote the paper; K. J. S. contributed to performing the research and to analysing the data.

The authors declare no conflict of interest.

¹To whom correspondence should be addressed. E-mail: df246cam.ac.uk

125 an energy), in which case the average of the function is not
 126 equal to the function of the average argument. In contrast,
 127 we consider the case where the probability to sample a point
 128 is given rigorously by the average of the stochastic estimator
 129 of the weight function.

130 To give a specific example, we consider the problem of
 131 computing the volume of the basin of attraction of a particular
 132 energy minimum i in a high-dimensional energy landscape (6–
 133 10). The algorithms developed in Refs. (6–9) rely on the fact
 134 that, for every point \mathbf{x} in a d -dimensional configuration space,
 135 we can determine unambiguously whether this point belongs
 136 to the basin of attraction of minimum i : if a (steepest-descent
 137 or similar) trajectory that start at point \mathbf{x} ends in minimum
 138 i , the ‘oracle function’ $\mathcal{O}_i(\mathbf{x}) = 1$, and otherwise it is zero.

139 However, many minimizers are not deterministic – and
 140 hence the oracle function is probabilistic. (In fact, historical
 141 evidence suggests that ancient oracles were probabilistic at
 142 best). In that case, if we start a number of minimisations at
 143 point \mathbf{x} , some will have $\mathcal{O}_i(\mathbf{x}) = 1$ and others have $\mathcal{O}_i(\mathbf{x}) = 0$.
 144 We denote with $P_{\mathcal{O}}^{(i)}(\mathbf{x})$ the average value of the Bernoulli
 145 process defined by the oracle function $\mathcal{O}_i(\mathbf{x})$. In words: $P_{\mathcal{O}}^{(i)}(\mathbf{x})$
 146 is the probability that the oracle function associated with point
 147 \mathbf{x} has a value of one.

148 We could obtain an estimate for the average weight $P_{\mathcal{O}}^{(i)}(\mathbf{x})$
 149 = $\langle \mathcal{O}^{(i)}(\mathbf{x}) \rangle$ by sampling the same point very many times.
 150 However, such an approach would be prohibitively expensive.
 151 Below we show that one can construct a rigorous algorithm
 152 to sample according to the weight $P_{\mathcal{O}}^{(i)}(\mathbf{x})$, without having to
 153 obtain an accurate estimate of $\langle \mathcal{O}^{(i)}(\mathbf{x}) \rangle$.

154 First, however, we generalise the concept of a basin volume
 155 v_i as the integral of the probability (the ‘probability mass’)
 156 that a stochastic minimization will end up in basin i .

$$157 \quad v_i \equiv \int d\mathbf{x} P_{\mathcal{O}}^{(i)}(\mathbf{x}) \quad [5]$$

160 Clearly, for a deterministic process, we recover the original
 161 definition of a basin volume. Moreover, we have

$$162 \quad \sum_{i=1}^{\Omega} v_i = V_{total} \quad [6]$$

165 where Ω is the number of distinct minima. This equation
 166 expresses the fact that every trajectory must end up somewhere.
 167 If we wish to compute the volume v_i in Eqn 5, we must be
 168 able to sample points with a probability $P_{\mathcal{O}}^{(i)}(\mathbf{x})$, even though
 169 we do not know this function *a priori*.

171 **Naive MC algorithm.** We will first describe a naive (and very
 172 inefficient), but rigorous MC algorithm to sample stochastic
 173 weight functions. After that, we will show how the algorithm
 174 can be made more efficient.

175 Our aim is to construct a MC algorithm that will visit points
 176 \mathbf{x} with a probability proportional to $P_{\mathcal{O}}(\mathbf{x})$. The normalized
 177 configuration-space density $\rho(\mathbf{x})$ is then proportional to $P_{\mathcal{O}}(\mathbf{x})$.
 178 If we can sample configuration space with this density $\rho(\mathbf{x})$,
 179 the computation of the volume in Eqn. 5 becomes a free-energy
 180 calculation, for which standard techniques exist (2).

181 Let us consider two points (\mathbf{x} and \mathbf{x}') between which we can
 182 carry out trial moves. The steady-state configuration-space
 183 density $\rho(\mathbf{x})$ is determined by our choice for the acceptance
 184 probability P_{acc} :

$$185 \quad \rho(\mathbf{x})P_{acc}(\mathbf{x} \rightarrow \mathbf{x}') = \rho(\mathbf{x}')P_{acc}(\mathbf{x}' \rightarrow \mathbf{x}) \quad [7]$$

The average acceptance probability for a very large number
 of trial moves from point \mathbf{x} to point \mathbf{x}' is $\langle \mathcal{O}(\mathbf{x}') \rangle = P_{\mathcal{O}}(\mathbf{x}')$.
 If we consider a large number of trial moves in the reverse
 direction, the acceptance probability is $P_{\mathcal{O}}(\mathbf{x})$. In steady state,
 the populations should be such that detailed balance holds
 and hence

$$192 \quad \rho(\mathbf{x})P_{\mathcal{O}}(\mathbf{x}') = \rho(\mathbf{x}')P_{\mathcal{O}}(\mathbf{x}) \quad [8]$$

or

$$194 \quad \frac{\rho(\mathbf{x})}{\rho(\mathbf{x}')} = \frac{P_{\mathcal{O}}(\mathbf{x})}{P_{\mathcal{O}}(\mathbf{x}')} \quad [9]$$

In other words: trial moves that are accepted with a proba-
 bility equal to the instantaneous value of the oracle function
 generate the correct distribution of points in configuration
 space, proportional to $P_{\mathcal{O}}(\mathbf{x})$.

Note that in this naive version of the algorithm, the accep-
 tance rule is not the Metropolis rule that considers the ratio of
 two weights. Here it is the probability itself. Hence, whenever
 the probability becomes very low, the acceptance of moves
 decreases proportionally. We address this problem in what
 follows.

‘Configurational-bias’ approach. With the naive algorithm de-
 scribed above, the acceptance of moves becomes small when
 the system moves into a region of configuration space where
 $P_{\mathcal{O}}(\mathbf{x})$ is low, and hence the ‘diffusion coefficient’ that de-
 termines the rate at which configuration space is sampled,
 becomes small. As a consequence, sampling of the wings of
 the distribution may become prohibitively slow. This problem
 can be alleviated by basing the Monte Carlo sampling on the
 average weight of a larger number of trial points. We do this
 by using an approach that resembles configurational bias MC
 (CBMC) (11), but is different in some respects. The key
 point to note is that, if we know all random numbers that
 determine the value of the oracle function – including the
 random numbers that control the behaviour of the stochastic
 minimiser – then in the extended space of coordinates plus
 random numbers, the value of the oracle function is always
 the same for a given point.

We can then generate a random walk in this extended
 space, between points that are surrounded by a ‘cloud’ of k
 points where we compute the oracle function (at this stage k is
 arbitrary). We denote the central point (i.e. the one to which
 or from which moves are attempted) by \mathbf{x}_B , where ‘B’ stands
 for ‘backbone’. The reason for calling this point a ‘backbone’
 point is that we will be sampling the k points connected to it,
 but we will not compute the oracle function at the backbone
 point. Hence, \mathbf{x}_B may even be located in a region where the
 oracle function is strictly zero (see Fig. 1). We introduce these
 backbone points because it facilitates generating a random
 walk that satisfies detailed balance.

The coordinates of the k cloud points around \mathbf{x}_B are given
 by:

$$239 \quad \mathbf{x}_{B,i} = \mathbf{x}_B + \Delta_i \quad [10]$$

with $i = \{1, 2, \dots, k\}$. The vectors Δ are generated by some
 stochastic protocol: e.g. the vectors may be uniformly dis-
 tributed in a hypersphere with radius R_h . The precise choice
 of the protocol does not matter, as long as the rules are not
 changed during the simulation. For a fixed protocol, the set
 $\mathbf{x}_{B,i}$ is uniquely determined by a set of random numbers \mathcal{R}_B .
 Finally, we note that the value of the oracle function \mathcal{O}_i for
 a given point $\mathbf{x}_{B,i}$ is uniquely determined by another set of

249 random numbers $\mathcal{R}_{\mathcal{O}}$ (e.g. the random numbers in a stochastic
250 minimisation).

251 We now define an extended state space

$$252 \quad \tilde{\mathbf{x}}_{\mathbf{B}} \equiv \{\mathbf{x}_{\mathbf{B}}, \mathcal{R}_{\mathbf{B}}, \mathcal{R}_{\mathcal{O}}\}. \quad [11]$$

254 In this space, the oracle functions are no longer fluctuating
255 quantities.

256 We can now construct a MCMC to visit (but not sample)
257 backbone points. To this end, we compute the ‘Rosenbluth
258 weight’ of point $\tilde{\mathbf{x}}_{\mathbf{B}}$ as

$$260 \quad W(\tilde{\mathbf{x}}_{\mathbf{B}}) = \sum_{i=1}^k \mathcal{O}_i \omega_i, \quad [12]$$

263 where $\mathcal{O}_i \equiv \mathcal{O}(\tilde{\mathbf{x}}_{\mathbf{B},i})$ and $\omega_i \equiv \omega(\tilde{\mathbf{x}}_{\mathbf{B},i})$ denotes a (Boltzmann)
264 biasing factor. For unbiased sampling, $\omega_i=1$, but for biased
265 sampling, as is used for instance in thermodynamic integra-
266 tion (2, 6–9), other choices for ω_i can be used.

267 We can then construct a MCMC algorithm where the accep-
268 tance of a trial move from the ‘old’ $\tilde{\mathbf{x}}_{\mathbf{B}}^{(o)}$ to the ‘new’ $\tilde{\mathbf{x}}_{\mathbf{B}}^{(n)}$
269 is given by

$$271 \quad P_{\text{acc}}(o \rightarrow n) = \text{Min} \left\{ 1, \frac{W(\tilde{\mathbf{x}}_{\mathbf{B}}^{(n)})}{W(\tilde{\mathbf{x}}_{\mathbf{B}}^{(o)})} \right\} \quad [13]$$

274 As the probabilities to generate the trial directions for
275 forward and backward moves, and the generation of random
276 numbers that determine the value of the oracle function are also
277 uniform, the resulting MC algorithm satisfies super-detailed
278 balance (2, 11) and a given backbone point $\tilde{\mathbf{x}}_{\mathbf{B}}$ will be visited
279 with a probability proportional to $W(\tilde{\mathbf{x}}_{\mathbf{B}})$. It is important to
280 note that the acceptance rules for the Markov chain determine
281 transition probabilities between the back-bone points, but that
282 these points are never sampled. Below, we show that we only
283 sample the values of the observable quantities for the cloud
284 points.

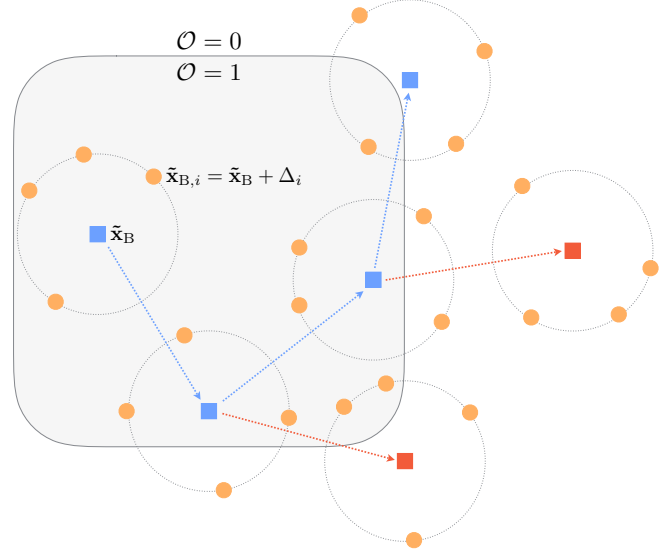
285 Note that during a trial move, the state of the old point is
286 not changed, hence it retains the same trial directions (hence
287 the same set $\{\mathcal{R}_{\mathbf{B}}\}$) and the same set $\{\mathcal{R}_{\mathcal{O}}\}$. If the trial move
288 is rejected, it is this ‘extended point’ that is sampled again.
289 This is different from standard CBMC.

290 The approach of Eq. 13 can be easily be incorporated in
291 more sophisticated sampling schemes such as Parallel Tem-
292 pering (PT) (12, 13), as discussed in the SI and shown in
293 Fig. 2.

295 **Sampling.** We have shown that backbone points will be visited
296 with a probability proportional to its instantaneous Rosenbluth
297 weight $P_{\mathbf{B}}(\tilde{\mathbf{x}}_{\mathbf{B}}) \sim W(\tilde{\mathbf{x}}_{\mathbf{B}})$. However, it is not our aim to sample
298 the backbone points but the points in the cloud around the
299 backbone. Let us consider two such points i_o and i_n that
300 belong to the cloud of the ‘old’ and ‘new’ of backbone points.
301 The condition for detailed balance states that the forward and
302 reverse fluxes between points i_o and i_n must balance:

$$303 \quad P(\tilde{\mathbf{x}}_{\mathbf{B}}^{(o)})P_{\text{gen}}(\tilde{\mathbf{x}}_{\mathbf{B}}^{(n)})P_{\text{sel}}(i_n)P_{\text{acc}}(o \rightarrow n) \\ 304 \quad = P(\tilde{\mathbf{x}}_{\mathbf{B}}^{(n)})P_{\text{gen}}(\tilde{\mathbf{x}}_{\mathbf{B}}^{(o)})P_{\text{sel}}(i_o)P_{\text{acc}}(n \rightarrow o), \quad [14]$$

307 where $P_{\text{sel}}(i_n)$ denotes the probability to select point i_n from
308 among the cloud of points around $\tilde{\mathbf{x}}_{\mathbf{B}}^{(n)}$ (and similarly, for
309 $P_{\text{sel}}(i_o)$). Note that this detailed balance condition comes on
310 top of the one for transitions between the backbone points,



311 **Fig. 1.** ‘Cloud’ sampling: illustration of the configurational-bias-like approach for a
312 simple oracle defined by the gray shaded region, such that $\mathcal{O} = 1$ inside the gray
313 boundary and $\mathcal{O} = 0$ outside. red and red squares denote typical accepted and
314 rejected backbone points $\tilde{\mathbf{x}}_{\mathbf{B}}$, respectively. The ‘cloud’ points $\tilde{\mathbf{x}}_{\mathbf{B},i} = \tilde{\mathbf{x}}_{\mathbf{B}} + \Delta_i$
315 are represented by orange circles. In this example we randomly sample $k = 4$ ‘cloud’
316 points from a circle of fixed radius centred on the backbone point (dotted circles).
317 Each ‘cloud’ is sampled with probability proportional to the Rosenbluth weight defined
318 in Eqn. 12. Note that backbone points (e.g. the one in the top right of the figure) may
319 fall outside the region where $\mathcal{O} = 1$ since the Rosenbluth weight (Eqn. 12) does not
320 depend on the value of the oracle at the backbone point.

321 which resulted in the acceptance rule 13 for the acceptance of
322 moves between those backbone points. In contrast, Eqn. 14
323 expresses the detailed balance condition for transitions be-
324 tween cloud points. In what follows, we will assume that the
325 probability $P_{\text{gen}}(\tilde{\mathbf{x}})$ to generate cloud points around a given
326 backbone point does not depend on $\tilde{\mathbf{x}}$. As a consequence, the
327 probabilities P_{gen} for forward and backward moves cancel, and
328 we shall drop P_{gen} from the detailed-balance equation.

329 To achieve the desired sampling of cloud points, we impose
330 that a given cloud point $i \equiv \mathbf{x}_{\mathbf{B},i}$ is selected with a probability

$$331 \quad P_{\text{sel}}(i) = \frac{\mathcal{O}(i)\omega(i)}{\sum_{j=1}^k \mathcal{O}(j)\omega(j)} = \frac{\mathcal{O}(i)\omega(i)}{W(\tilde{\mathbf{x}}_{\mathbf{B}})}. \quad [15]$$

332 If we now make use of the fact that the probability to visit
333 a given backbone point at $\tilde{\mathbf{x}}_{\mathbf{B}}$ is proportional to $W(\tilde{\mathbf{x}}_{\mathbf{B}})$, it
334 follows that the overall probability $P(i; \tilde{\mathbf{x}}_{\mathbf{B}})$ that point a cloud
335 point i will be sampled is proportional to the desired weight:

$$336 \quad P(i; \tilde{\mathbf{x}}_{\mathbf{B}}) \sim W(\tilde{\mathbf{x}}_{\mathbf{B}}) \frac{\mathcal{O}(i)\omega(i)}{W(\tilde{\mathbf{x}}_{\mathbf{B}})} = \mathcal{O}(i)\omega(i).$$

337 But note that $\mathcal{O}(i)$ has not yet been averaged. If we perform
338 the average over the oracle function, we obtain:

$$339 \quad P(i) \sim \langle \mathcal{O}(i) \rangle \omega(i).$$

340 Hence, by combining our rule for visiting backbone points
341 with a Rosenbluth style selection of the point to be sampled,
342 we ensure that we sample with the correct weight.

343 The approach that we describe here is better than the naive
344 algorithm because it achieves faster ‘diffusion’ through parts
345 of configuration space where $\langle \mathcal{O} \rangle \omega$ is small.

373 However, even though Rosenbluth-style sampling ensures
 374 that all points in space are sampled with the correct frequency,
 375 it is not an efficient algorithm. The reason is obvious: in
 376 order to compute the weights W , the oracle function must be
 377 computed for k points, and yet in naive Rosenbluth sampling,
 378 only one point would be sampled.

379 Fortunately, this drawback can be overcome. Rather than
 380 sampling one point at a time, we take steps between backbone
 381 points sampled according to Eqn. 13 and compute the quantity
 382 to be sampled for all k cloud points belonging to the current
 383 backbone point, as described below. An illustration of the
 384 method is given in Fig. 1.

385 For every backbone point $\tilde{\mathbf{x}}_B$ visited, we can compute the
 386 observable (say A) of the set of k cloud points as follows:

$$387 A_{\text{sampled}} = \frac{\sum_{i=1}^k \mathcal{O}_i \omega_i A_i}{\sum_{i=1}^k \mathcal{O}_i \omega_i} \quad [16]$$

390 The average of A during a MCMC simulation of L steps is:

$$391 \frac{1}{L} \sum_{j=1}^L \left(\frac{\sum_{i=1}^k \mathcal{O}_i \omega_i A_i}{\sum_{i=1}^k \mathcal{O}_i \omega_i} \right)_j \quad [17]$$

396 where the index j labels the different backbone states visited.

397 **Combine with ‘Waste-recycling’ MC.** Efficiency can be further
 398 improved by using the approach underlying ‘waste-recycling’
 399 Monte Carlo (14). This approach allows us to sample all
 400 points trial cloud points in the sampling, even if the actual
 401 trial backbone move is rejected. The approach of ref. (14)
 402 allows us to combine the information of the accepted and the
 403 rejected states in our sampling. Specifically, we denote the
 404 probability to accept a move from an old state o to a new state
 405 n by $P'_{\text{acc}}(o \rightarrow n)$, then, normally we would sample $A_{\text{sampled}}(n)$
 406 if the move is accepted and $A_{\text{sampled}}(o)$ otherwise. However,
 407 we can do better by combining the information and sample

$$408 A_{\text{wr}} = P'_{\text{acc}}(o \rightarrow n) A_{\text{sampled}}(n) + [1 - P'_{\text{acc}}(o \rightarrow n)] A_{\text{sampled}}(o) \quad [18]$$

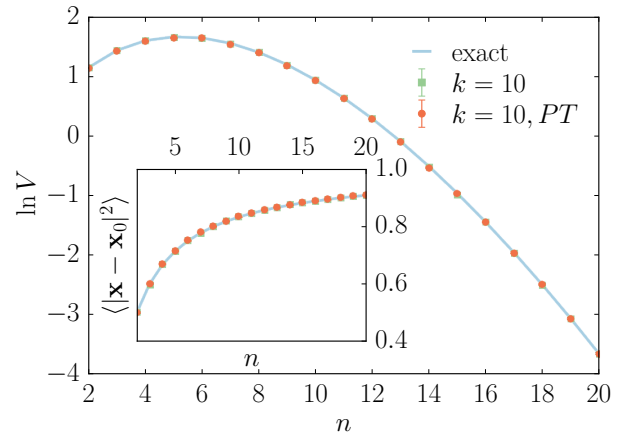
409 where P'_{acc} denotes the acceptance probability for *any* valid
 410 MCMC algorithm (not just Metropolis). In fact, it is convenient
 411 to use the symmetric (Barker) rule (15) to compute P'_{acc} .
 412 In that case, we would sample

$$413 A_{\text{wr}} = \frac{\left(\sum_{i=1}^k \mathcal{O}_i \omega_i A_i \right)_{\text{old}} + \left(\sum_{i=1}^k \mathcal{O}_i \omega_i A_i \right)_{\text{new}}}{\left(\sum_{i=1}^k \mathcal{O}_i \omega_i \right)_{\text{old}} + \left(\sum_{i=1}^k \mathcal{O}_i \omega_i \right)_{\text{new}}} \quad [19]$$

420 Hence, all $2k$ points that have been considered are included
 421 in the sampling.

422 Numerical Results

423 **Basin volume calculations.** To test the proposed algorithm we
 424 compute the basin volume (probability mass) for a stochastic
 425 oracle function as defined in Eqn. 5. We choose a few simple
 426 oracle functions, for which the integral in Eqn. 5 can be solved
 427 analytically. The volume calculations were performed using the
 428 multi-state-Bennett acceptance ratio method (MBAR) (16)
 429 as described in Ref. (9). As described in Ref. (9), a high-
 430 dimensional volume calculation is in essence a free-energy
 431 calculation, where minus the log of the volume plays the role
 432 of the free energy.



435 **Fig. 2.** Deterministic oracle: Volume calculation for an n -dimensional hypersphere
 436 with radius $R = 0.5$ and $n \in [2, 20]$. Numerical results (symbols) were obtained by
 437 the configurational bias approach of Eqn. 13, with k ‘cloud’ points, and MBAR. PT
 438 refers calculations performed by Parallel Tempering, described in the SI. Inset: mean
 439 square displacement computed by Eqn. 17. Solid red lines are analytical results and
 440 error bars refer to twice the standard error (as estimated by MBAR for the volume).
 441

442 We compute the dimensionless free energy difference between a region of known volume
 443 $\hat{f}_{\text{ref}} = -\ln V_{\text{ref}} + c$ and the equilibrium distribution of points sampled uniformly within
 444 the basin $\hat{f}_{\text{tot}} = -\ln V_{\text{tot}} + c$, estimated by MBAR up to an additive constant c . Since
 445 $f_{\text{ref}} = -\ln V_{\text{ref}}$ is known, we obtain the basin volume as $f_{\text{tot}} = f_{\text{ref}} + (\hat{f}_{\text{tot}} - \hat{f}_{\text{ref}})$. We use 15
 446 replicas with positive coupling constants for all examples discussed herein, see Ref. (9)
 447 for details of the method.

448 We first tested the method for a deterministic oracle, namely a simple n -dimensional
 449 hypersphere of known volume $V_{n\text{-ball}} = \pi^{n/2} R^n / \Gamma(n/2 + 1)$ with radius $R = 0.5$
 450 and $n \in [2, 20]$. As shown in Fig. 2 we correctly recover the volume and the mean
 451 square displacement using the acceptance rule defined in Eqn. 13 for $k = 10$ ‘cloud’
 452 points. The figure suggests that the algorithm is sampling the correct equilibrium
 453 distributions.

454 Next, we tested the method for a stochastic oracle function defined such that

$$455 P_{\mathcal{O}}(\mathbf{x}) \sim \begin{cases} 1 & \text{if } |\mathbf{x}| < R \\ \exp[-(|\mathbf{x}| - R)/\lambda] & \text{if } |\mathbf{x}| \geq R \end{cases} \quad [20]$$

456 with volume

$$457 V = 2(R^n/n + \lambda^n \exp(R/\lambda) \Gamma(n, R/\lambda)) \pi^{n/2} R^n / \Gamma(n/2),$$

458 where $\Gamma(a, x)$ is the incomplete gamma function. Results for dimensions $n \in [2, 20]$,
 459 $R = 0.5$ and $\lambda = 0.1$ are shown in Fig. 3. Note that, despite the volume being finite,
 460 the basin is unbounded in the sense that the average value of the oracle only tends
 461 to zero as $|\mathbf{x}| \rightarrow \infty$. As the dimensionality of the basin increases, all of the
 462 volume will concentrate away from the centre of mass in regions of space where the
 463 oracle has a high probability of returning 0. Hence, it becomes more difficult
 464 for a random walker to diffuse efficiently as the dimensionality of space increases.
 465 We can verify this in Fig. 3: for $n < 6$ results seem to be independent of the
 466 number of ‘cloud’ points. However, growing deviations are observed for increasing
 467 n and accuracy increases significantly for growing number of

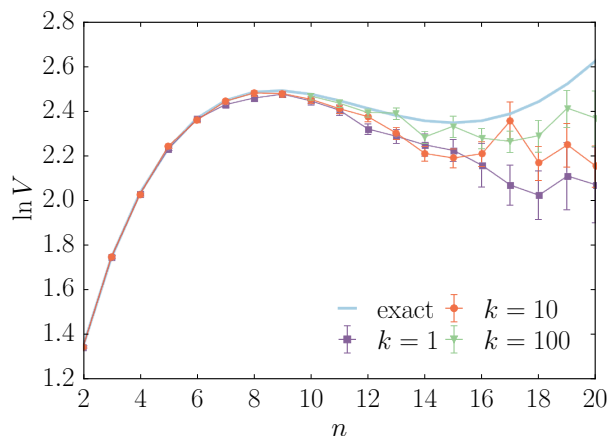


Fig. 3. Stochastic oracle: Volume calculation for the oracle defined in Eqn. 20 with radius $R = 0.5$, $\lambda = 0.1$ and dimensions $n \in [2, 20]$. Symbols (lines are guide to the eye) are numerical results obtained by the configurational bias approach of Eqn. 13 with k ‘cloud’ points, and MBAR. The light blue curve denotes the analytical results and error bars refer to twice the standard error as estimated by MBAR. At large n accuracy increases by increasing k as the random walker diffuses more efficiently through regions of space where $\langle \mathcal{O} \rangle \ll 1$. However, if the integral is dominated by points where the average value of the oracle function is (much) less than the inverse of the number of cloud points, slow convergence leads to systematic errors in the sampling.

‘cloud’ points k . For large n , the largest contribution to the integral comes from values of $|x|$ where the average value of the oracle function is very small ($\mathcal{O}(10^{-9})$ for $n = 20$). We carried out our simulations with at most 100 cloud points. In that case, inefficient sampling could be expected when the average oracle function is significantly less than 0.01. As the figure shows, for the case of $k = 100$ systematic deviations from the analytical result show up for $n \geq 11$, where the dominant contributions come from points where the average oracle function is $\mathcal{O}(10^{-5})$.

Transition state finding. The algorithm that we described above has wider applicability than the specific examples that we discussed. As an illustration of a very different application, we show that our approach can be used to efficiently identify the transition state along a known reaction coordinate.

Note that points in the transition-state ensemble (in the one-dimensional case: just one point) are characterised by the property that the committer has an average value of 0.5. However, any individual trajectory will either be crossing (‘1’) or non-crossing (‘0’). Hence, the ‘signal’ is stochastic. As an illustration, we consider the (trivial) one-dimensional case of a particle with kinetic energy K sampled according to the 1-dimensional Maxwell Boltzmann distribution, crossing a Gaussian barrier with height $U_{\text{tr}} = 30kT$ and variance $\sigma^2 = 1$. We define the oracle symmetrically such as

$$\mathcal{O}(x) = \begin{cases} 1 & \text{if } K > U_{\text{tr}} - U(x) \\ 0 & \text{if } K \leq U_{\text{tr}} - U(x) \end{cases} \quad [21]$$

and constrain the walk to reject moves for which the potential energy is below that of the initial position, such that $\mathcal{O} = 0$ if $U(x) < U(x_0)$; we choose $x_0 = 2\sigma$. By thus constraining the

*We choose as our unit of length σ , hence in our reduced units $kT = \sigma^2$

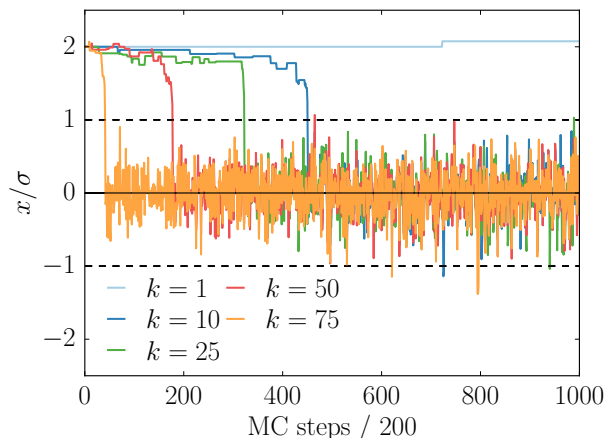


Fig. 4. Transition state finding: the simple case of one dimensional barrier crossing is defined (symmetrically) by the stochastic oracle in Eqn. 21. A series of random walks are performed according to Eqn. 13 with different number of ‘cloud’ points k . The walkers are constrained to reject moves for which the energy is below that of the initial position, thus excluding reactants and products from the sampling. The figure shows the position of the walker backbone along the reaction coordinate as a function of the number of MCMC steps. For increasing k the random walkers diffuse more efficiently and therefore converge faster to the transition state. Traditional single-point sampling does not move at all from the initial condition.

sampling, we are excluding the ‘reactant’ and ‘product’ states from our sampling. In Fig. 4 we show results for backbone step-size 0.25σ , ‘cloud’ radius 0.25σ and varying number of ‘cloud’ points k . One can clearly see that as the number of ‘cloud’ points increases the system diffuses faster towards the transition state whilst for the traditional single-point sampling the walker does not move at all from the initial position.

Relation to earlier work

The problem of Monte Carlo sampling in the presence of noise has been discussed by Bhanot and Kennedy (4) and Ceperley and Dewing (5).

Bhanot and Kennedy (4) considered how to construct an unbiased estimator of an exponential function (e.g. a ratio of Boltzmann weights) with a fluctuating argument. This method involves constructing an estimator on the basis of a number of independent samples. The method is subject to certain limitations (it is not guaranteed to generate acceptance probabilities between 0 and 1) and, crucially, it addresses the problem that the average of an exponential function with fluctuating argument is not equal to the function of the average argument. In this respect, the work of ref. (4) is similar to that of Ceperley and Dewing (5) who considered the problem of performing Boltzmann MCMC sampling in cases where the energy function is noisy. As in the case of ref. (4), the Boltzmann weight is a nonlinear function of the energy and that therefore the Boltzmann factor corresponding to the average energy is not the same as the average of the Boltzmann factor obtained by sampling over energy fluctuations. Specifically, Ceperley and Dewing (5) consider the case where the calculation of the energy function is subject to statistical errors with zero mean. In that case, we cannot use the conventional Metropolis rule $P_{\text{acc}} = \text{Min}\{1, \exp(-\beta\Delta u)\}$, where u is the instantaneous value of the energy difference, because what is needed to com-

621 pute the correct acceptance probability is $\exp(-\beta\langle\Delta u\rangle)$, but
 622 what is sampled is $\langle\exp(-\beta\Delta u)\rangle \neq \exp(-\beta\langle\Delta u\rangle)$. Ceperley
 623 and Dewing showed that if the fluctuations in Δu are normally
 624 distributed, with constant variance σ , then we can still get an
 625 algorithm that samples the correct Boltzmann distribution, if
 626 we use as acceptance rule

$$627 \quad P_{\text{acc}} = \text{Min}\{1, \exp[-\beta\Delta u - (\beta\sigma)^2/2]\} \quad [22]$$

630 Note that the situation considered in Refs. (4) and (5)
 631 is very different from the case that we consider here, as we
 632 focus on the situations where the average of the (fluctuating)
 633 oracle functions is precisely the weight function that we wish
 634 to sample. However, the current approach allows us to re-
 635 derive the Ceperley-Dewing result. We note that, as before,
 636 we can consider extended states characterised by the spatial
 637 coordinates of the system and by the random variables that
 638 characterise the noise in the energy function. To discuss the
 639 approach of Ceperley and Dewing in the present language, it
 640 is easiest to consider the case that the variance in the energy
 641 of the individual states is normally distributed, with constant
 642 variance σ_s . The average Boltzmann factor of extended state
 643 i is then

$$644 \quad \langle P_i \rangle = \exp[-\beta\langle u \rangle_i] \exp[(\beta\sigma_s)^2/2] \quad [23]$$

645 and therefore

$$646 \quad \frac{\langle P_n \rangle}{\langle P_o \rangle} = \exp[-\beta\langle\Delta u\rangle] \quad [24]$$

649 Hence, the average Boltzmann factor of any state i is still
 650 proportional to the correct Boltzmann weight. However, an
 651 MCMC algorithm using the instantaneous Boltzmann weights
 652 would not lead to correct sampling as super-detailed balance
 653 yields

$$654 \quad \frac{P_n(\mathbf{x}_n)}{P_o(\mathbf{x}_o)} = \exp[-\beta\Delta u] \quad [25]$$

655 and hence

$$656 \quad \left\langle \frac{P_n}{P_o} \right\rangle = \exp[-\beta\langle\Delta u\rangle + (\beta\sigma)^2/2] \quad [26]$$

661 which is not equal to

$$662 \quad \frac{\langle P_n \rangle}{\langle P_o \rangle} = \exp[-\beta\langle\Delta u\rangle] \quad [27]$$

- 667 1. Manousiouthakis V, Deem M (1999) Strict detailed balance is unnecessary in monte carlo simulation. *J. Chem. Phys.* 110:2753–2756.
- 668 2. Frenkel D, Smit B (2002) *Understanding molecular simulation*. (Academic Press, San Diego).
- 669 3. Metropolis N, Rosenbluth AW, Rosenbluth MN, Teller AH, Teller E (1953) Equation of state calculations by fast computing machines. *J. Chem. Phys.* 21:1087–1092.
- 670 4. Bhanot G, Kennedy A (1985) Bosonic lattice gauge theory with noise. *Phys. Lett.* 157B:70–76.
- 671 5. Ceperley D, Dewing M (1999) The penalty method for random walks with uncertain energies. *J. Chem. Phys.* 110:9812–9820.
- 672 6. Xu N, Frenkel D, Liu AJ (2011) Direct determination of the size of basins of attraction of jammed solids. *Phys. Rev. Lett.* 106:245502.
- 673 7. Asenjo D, Paillusson F, Frenkel D (2014) Numerical calculation of granular entropy. *Phys. Rev. Lett.* 112:098002.
- 674 8. Martiniani S, Schrenk K, Stevenson J, Wales D, Frenkel D (2016) Turning intractable counting into sampling: Computing the configurational entropy of three-dimensional jammed packings. *Phys. Rev. E* 93:012906.
- 675 9. Martiniani S, Schrenk K, Stevenson J, DJ W, Frenkel D (2016) Structural analysis of high-dimensional basins of attraction. *Phys. Rev. E* 94:031301.
- 676 10. Martiniani S, Schrenk K, Ramola K, Chakraborty B, Frenkel D (2017) Numerical test of the edwards conjecture shows that all packings become equally probable at jamming. *Nature Physics* 17:xxx.

683 If, however we would use the Ceperley-Dewing acceptance rule,
 684 we would get

$$685 \quad \left\langle \frac{P_n}{P_o} \right\rangle = \exp[-\beta\langle\Delta u\rangle + (\beta\sigma)^2/2] \times \exp[-(\beta\sigma)^2/2] \quad [28]$$

$$686 \quad = \exp[-\beta\langle\Delta u\rangle] = \frac{\langle P_n \rangle}{\langle P_o \rangle}$$

689 Hence, with this rule the states would (on average) be visited
 690 with the correct probability. Note that, as the noise enters non-
 691 linearly in the acceptance rule, the Ceperley-Dewing algorithm
 692 is very different from the one that we derived above. Note also
 693 that the present derivation makes it clear that the Ceperley-
 694 Dewing algorithm can be easily generalised to cases where the
 695 noise in the energy is not normally distributed, as long as the
 696 distribution of the noise is state-independent.

697 Conclusions and outlook

698 Thus far the algorithm described above was presented as a
 699 method to perform Monte Carlo sampling in cases where the
 700 weight function itself is fluctuating.

701 However, we suggest that the method is not limited to
 702 numerical sampling: it could be used to steer sampling of
 703 experimental control parameters in experiments that study
 704 stochastic events (e.g. crystal nucleation, cell death or even
 705 the effect of advertising). Often, the occurrence of the desired
 706 event depends on a large number of variables (temperature,
 707 pressure, pH , concentration of various components) and we
 708 would like to select the optimal combination. However, as
 709 the desired event itself is stochastic, individual measurements
 710 provide little guidance. One might aim to optimise the condi-
 711 tions by accumulating sufficient statistics for individual state
 712 points. However, such an approach is expensive. The proce-
 713 dure described in the preceding sections suggests that it may
 714 be better to perform experiments in a ‘cloud’ of state points
 715 around a backbone point. We could then accept or reject the
 716 trial move to a new backbone state using the same rule as in
 717 Eqn. 13. In this way, the experiment could be made to evolve
 718 towards ‘interesting’ regions of parameter space.

719 **ACKNOWLEDGMENTS.** D. F. acknowledges support by EPSRC
 720 Programme Grant EP/I001352/1 and EPSRC grant EP/I000844/1.
 721 K. J. S. acknowledges support by the Swiss National Science Founda-
 722 tion (Grant No. P2EZP2-152188 and No. P300P2-161078). S. M.
 723 acknowledges financial support from the Gates Cambridge Scholar-
 724 ship.

- 725 11. Frenkel D, Mooij G, Smit B (1991) Novel monte carlo scheme to study structural and thermal properties of continuously deformable molecules. *J. Phys. Condensed Matt.* 3:3053–3076.
- 726 12. Lyubartsev A, Martisnovski A, Shevkunov S, Vorontsov-Velyaminov P (1992) New approach to Monte Carlo calculation of the free energy: Method of expanded ensembles. *J. Chem. Phys.* 96:1776.
- 727 13. Marinari E, Parisi G (1992) Simulated tempering: a new Monte Carlo scheme. *Europophys. Lett.* 19:451–458.
- 728 14. Frenkel D (2004) Speed up of monte carlo simulations by sampling of rejected states. *Proc. Nat. Acad. Sci. USA* 101:17571–17575.
- 729 15. Barker A (1965) Monte carlo calculations of radial distribution functions for a proton-electron plasma. *Aust. J. Phys.* 18:119–133.
- 730 16. Shirts MR, Chodera JD (2008) Statistically optimal analysis of samples from multiple equilibrium states. *J. Chem. Phys.* 129:124105.
- 731 17. Yan Q, de Pablo J (1999) Hyper-parallel tempering Monte Carlo: Application to the Lennard-Jones fluid and the restricted primitive model. *Journal of Chemical Physics* 111:9509–9516.
- 732 18. Bunker A, Dünweg B (2000) Parallel excluded volume tempering for polymer melts. *Phys. Rev. E* 63:016701.
- 733 19. Fukunishi H, Watanabe O, Takada S (2002) On the Hamiltonian replica exchange method for efficient sampling of biomolecular systems: Application to protein structure prediction. *J. Chem. Phys.* 116:9058.

Supplementary Information: Monte Carlo sampling for stochastic weight functions

Frenkel et al. 10.1073/pnas.XXXXXXXXXX

Parallel Tempering

Parallel Tempering (PT) (12, 13) is a Monte Carlo scheme that targets the slow equilibration of systems characterised by large free energy barriers that prevent the efficient equilibration of a MCMC random walk. In PT, m replicas of the system are simulated simultaneously at different temperatures, different chemical potentials (17) or different Hamiltonians (18, 19). Configurations are then swapped among replicas, thus making ‘high temperature’ regions available to ‘low temperature’ ones and *vice versa*. In the basin volume calculations of Refs. (7, 8, 9, 10), Hamiltonian PT is essential to achieving fast equilibration of the replicas’ MCMC random walks performed inside the body of the basin with different applied biases.

The configurational bias approach to ‘cloud’ sampling embodied by Eqn. 13 can be easily generalised to PT to find an acceptance rule for the swap of configurations between replicas i and j

$$P_{\text{acc}}(i \rightarrow j) = \text{Min} \left\{ 1, \frac{W(\tilde{\mathbf{x}}_{\text{B}}^{(i)}, \omega^{(j)})W(\tilde{\mathbf{x}}_{\text{B}}^{(j)}, \omega^{(i)})}{W(\tilde{\mathbf{x}}_{\text{B}}^{(i)}, \omega^{(i)})W(\tilde{\mathbf{x}}_{\text{B}}^{(j)}, \omega^{(j)})} \right\} \quad [\text{S1}]$$

where we defined the Rosenbluth weight $W(\tilde{\mathbf{x}}_{\text{B}}^{(i)}, \omega^{(j)}) = \sum_{l=1}^k \mathcal{O}(\tilde{\mathbf{x}}_{\text{B},l}^{(i)})\omega^{(j)}(\tilde{\mathbf{x}}_{\text{B},l}^{(i)})$. It is important to note that PT is truly an equilibrium Monte Carlo method: the microscopic equilibrium of each ensemble is not disturbed by the swaps.

We have tested this method both for a deterministic oracle – a simple n -dimensional hypersphere – shown in Fig. 2 of the main text, and for the stochastic oracle defined in Eq. 20 as

shown in Fig. S1 (compare to Fig. 3 of the main text).

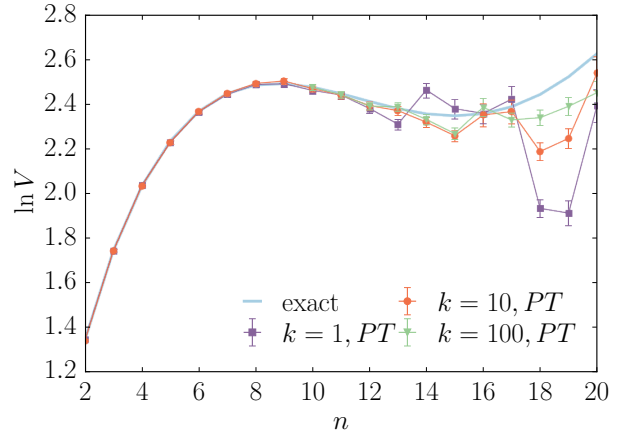


Fig. S1. Stochastic oracle: Volume calculation for the oracle defined in Eqn. 20 with radius $R = 0.5$, $\lambda = 0.1$ and dimensions $n \in [2, 20]$. Symbols (lines are guide to the eye) are numerical results obtained by the configurational bias approach of Eqn. S1 with k ‘cloud’ points, and MBAR, compare to Fig. 3 of the main text. The light blue curve denotes the analytical results and error bars refer to twice the standard error as estimated by MBAR. At large n accuracy increases by increasing k as the random walker diffuses more efficiently through regions of space where $\langle \mathcal{O} \rangle \ll 1$. However, if the integral is dominated by points where the average value of the oracle function is (much) less than the inverse of the number of cloud points, slow convergence leads to systematic errors in the sampling.